Pergamon

PII: S0360-5442(97)00017-0

Energy Vol. 22, No. 9, pp. 875–885, 1997

Printed in Great Britain
0360-5442/97 $17.00 + 0.00

SIMULATION AND EXERGY ANALYSIS OF TRANSIENT DIESEL-ENGINE OPERATION

C. D. RAKOPOULOS† and E. G. GIAKOUMIS

Internal Combustion Engines Laboratory, Thermal Engineering Section, Mechanical Engineering Department, National Technical University of Athens, 42 Patission Str., Athens 10682, Greece

(Received 4 October 1996)

Abstract—A computer analysis has been developed for studying the energy and exergy performance of an indirect-injection, naturally-aspirated diesel engine operating under transient load or speed conditions and covering the operating profile of both industrial and automotive engines. The model is validated at steady-state operation and incorporates many novel features for simulating the transient response and analyzing all of the engine availability terms. The analysis reveals via multiple diagrams how the exergy properties of the diesel-engine subsystems vary according to the engine cycles for various speed and load changes. The diagrams also show the current-speed response. In addition, the effects of operating parameters such as the intensity of the applied change or heat loss to the walls are described from first- and second-law perspectives. © 1997 Elsevier Science Ltd.

INTRODUCTION

Diesel-engine simulation modelling has long been established as an effective tool for studying engine performance and contributing to evaluation and new developments. Thermodynamic models of the real diesel-engine cycle [1–5] have served as a sound basis for complete analysis of engine performance and sensitivity to various operating parameters. Transient response, especially of turbocharged and naturally aspirated compression–ignition (diesel) engines, forms a significant part of their operation; it is characterized by short but serious off-design functions, requiring careful and proper modelling for successful study of the (speed) response [6–12]. Moreover, during the last 20 years, it has become clear that first-law theory alone, even when properly applied, often fails to provide adequate insight into engine operations [13–16]. By contrast, second-law (exergy or availability) analysis with detailed study of what is happening during a process has contributed a new way of thinking about and studying thermodynamic processes [5,17–22].

In the present study, we describe improved simulation of transient operations. Our simulation includes innovations such as detailed analysis of thermodynamic and dynamic differential equations which account for the continuously changing character of transient operations, a more complete analysis than is given in earlier treatments of transient mechanical friction, combustion and fuel injection, as well as detailed modelling of engine-inertia forces and incorporation of a fully mathematical model of the (direct-acting) governor. Experimental results have been used under a variety of steady-state operating conditions to obtain calibration constants. An exergy balance is applied to all subsystems of the diesel engine such as the cylinder for both the closed and open parts of the cycle and the inlet and exhaust manifolds. We describe how the exergy changes (work, heat transfer, exhaust gas, irreversibilities) develop during a transient event. This is an original feature since second-law analysis has only been applied in the past to steady-state diesel-engine operations. Both speed and load-change operating schedules have been studied. Furthermore, the effects of important operating parameters such as the intensity of the applied (speed or load) change and heat losses to the walls are investigated with the help of explicit multiple diagrams which show the speed profiles of transient events together with the most significant energy and exergy changes in the engine.

†Author for correspondence. Fax: (30)-1-772-3475.

ENERGY ANALYSIS

General process description

There is spatial uniformity of pressure, temperature and composition in the combustion chamber at each instant of time (single-zone model). The fuel is dodecane ($C_{12}H_{26}$) with an LHV = 42,500 kJ/kg. We assume perfect gas behavior [23]. Polynomial expressions proposed by Krieger and Borman [24] are used for each of the four species (O_2, N_2, CO_2, and H_2O) considered in evaluations of internal energy and specific heats for first-law applications to the engine cylinder contents [1–5,11,24].

Fuel pump and injection

To simulate the fuel-injection rate $\dot{m}_{fi}$ (kg/s), the following expression proposed by Ferguson [1] is used:

$$\frac{\dot{m}_{fi}}{M_{tot}} = \frac{\omega(\varphi)}{\varphi_d \Gamma(n)} \left(\frac{\varphi - \varphi_s}{\varphi_d}\right)^{n-1} \exp\left(\frac{\varphi_s - \varphi}{\varphi_d}\right), \tag{1}$$

where $\ln\Gamma(n) = (n - 0.5)\ln(n) - n + 0.5\ln(2\pi) + 1/(12n) - 1/(360n^3) + 1/(1260n^5)$ with $n = 3.6$. Here, φ_s is the crank angle where injection begins, φ_d the duration of injection, and M_{tot} the total amount of injected fuel per cycle, which is found by using experimental data under steady-state conditions for the applicable engine-speed and fuel-pump rack position.

Combustion

For the study of combustion processes, the model proposed by Whitehouse and Way is used [3–5,8], i.e we include preparation-limited and reaction-limited combustion rates. The corresponding equations are

$$P = K_1 M_i^{1-x} M_u^x p_O^y \text{ (kg of fuel per°CA)} \tag{2a}$$

for the preparation rate, which controls the rate of burning of most of the fuel, and

$$R = (K_2 p_O / N\sqrt{T}) e^{-\mathrm{act}/T} \int (P - R) d\varphi \text{(kg of fuel per°CA)} \tag{2b}$$

for the rate responsible for the early part of combustion. Here, $M_i - \int_{\varphi_s}^{\varphi} (dm_{fi}/d\varphi) d\varphi$ is the total mass (kg) of injected fuel up to the crank angle φ and $(dm_{fi}/d\varphi)$ is the injection rate known from Eq. (1). Also, $M_u = M_i - \int P d\varphi$ is the total mass (kg) of unprepared fuel, act is the reduced activation temperature (K) which accounts for the ignition delay, and p_O is the partial pressure of oxygen (bars). The constants x, y, K_1, and K_2 are found from calibrations against experimental data under steady-state conditions.

It is vital for proper simulation of transient responses that combustion modelling takes into account the continuously changing character of the operating conditions. The constant K_1 in the (dominant) preparation-rate equation is correlated with the Sauter mean diameter (*SMD*) of the fuel droplets by the relation $K_1 \propto (1/SMD)^2$. The empirical expression of Hiroyasu et al [2] is used, i.e.

$$SMD = 23.9(\Delta p)^{-0.135} \rho_g^{0.12} V_{tot}^{0.131} (\mu m), \tag{3}$$

where ΔP is the mean pressure drop across the injection nozzle in MPa, ρ_g the air density in kg/m^3 at the beginning of injection, and V_{tot} (in mm^3) is the amount of fuel delivered per cycle per pump stroke.

Heat transfer

The model of Annand [3,8] is used to simulate heat loss to the cylinder walls, viz.,

$$dQ_L/dt = F[a(\lambda/D)\mathrm{Re}^b(T_w - T_g) + c(T_w^4 - T_g^4)], \tag{4}$$

where $F = \pi D^2/4 + \pi Dx$ is the surface and x the instantaneous cylinder height in contact with the gas;

λ is the gas thermal conductivity (W/mK) and the Reynolds number Re is calculated with a characteristic speed equal to the mean piston speed and a characteristic length equal to the piston diameter D. For transient engine operation, an hysterysis expression is used to update the wall temperature T_w at each consecutive cycle, which changes as a result of the increase in speed and/or fuelling [11].

Mechanical friction

To calculate the friction inside the cylinder, the following expression of Millington and Hartles [25] is used:

$$(fmep)_{st} = 0.123CR + 4.774 \times 10^{-4}N, \tag{5}$$

where $(fmep)_{st}$ is the friction mean effective pressure (bar) at steady-state conditions and CR is the engine compression ratio.

For transient operations, we use the relation

$$(fmep)_{tr} = (fmep)_{st}[1 + c_{fr}|\epsilon/\epsilon_{max}|], \tag{6}$$

where ϵ stands for the current angular acceleration (mean value over the engine cycle) and ϵ_{max} is the maximum angular acceleration (or deceleration) which is experienced due to a 0–100% load increase (or decrease) during one cycle. The constant $c_{fr} = 0.5$ to make the results agree with a proposal by Winterbone [8].

DYNAMIC ANALYSIS

Engine dynamics

If G_{tot} (in kg-m^2) represents the total system moment of inertia (engine, flywheel, and load), then the conservation of energy principle applied to the total system (engine plus load) is [2,11]

$$T_e(\varphi,\omega) - T_L(\omega) - T_{fr} = G_{tot}(d\omega/dt). \tag{7}$$

Here, $T_e(\varphi,\omega)$ stands for the instantaneous value of the engine torque, which is the sum of the gas and inertial forces torque, i.e. [11,26]

$$T_e(\varphi,\omega) = [p_g(\varphi)F_pR_1 + N_{T_{in}}]r, \tag{8}$$

where $p_g(\varphi)$ is the instantaneous gas pressure, F_p the piston cross-sectional area = $\pi D^2/4$, R_1 a measure of the instantaneous piston velocity [11], and $N_{T_{in}}$ the force acting on the piston due to the inertia of the moving parts (piston and a part of the connecting rod) with the complex movement of the rod taken into consideration [11]. In Eq. (7), the load torque is

$$T_L(\omega) = \tau + k\omega^s. \tag{9}$$

For the cases that will be analyzed, the load is either linear (electric brake) so that $\tau = 0$, $s = 1$ and $k>0$ or rigid (automotive applications) with $\tau \neq 0$ and $k = 0$.

In Eq. (7), T_{fr} stands for the friction term, which is constant during each cycle and is related to the transient friction mean effective pressure $(fmep)_{tr}$ by the expression

$$T_{fr} = [(fmep)_{tr}/2\pi]F_pr. \tag{10}$$

Governor dynamics

A mechanical governor is simulated in the present analysis. It operates according to Watt's principle. During transient operation, Newton's second law of motion for the sensing element of the governor (on a °CA basis) is [11,27,28]

$$m_{gov}\omega^2(d^2z/d\varphi^2) + f\omega(dz/d\varphi) + (k - b_{se}\omega_{gov}^2)z = a_{se}\omega_{gov}^2 - ky_0, \tag{11}$$

where z is the current displacement of the governor clutch (equal to the spring deformation), f the clutch friction coefficient (Ns/m), m_{gov} the combined mass of the clutch and flyweights, k the governor spring stiffness (N/m), a_{se} and b_{se} are characteristic properties of the governor sensing element [11,27], and y_0 is the prior governor spring strain (also known as the governor setting).

EXERGY ANALYSIS

The availability or exergy of a system in a given state is defined as the maximum reversible work that can be produced through interaction of the system with its surroundings as it reaches thermal, mechanical and chemical equilibrium [13,29–32]. In this study, only thermal and mechanical availability terms are taken into account, while chemical availability is involved only in the reactions of fuels to form products.

Application of the exergy-balance equation to diesel-engine subsystems, on a °CA basis, yields the relations given in the three succeeding paragraphs [5,22]:

For the cylinder,

$$dA_{cyl}/d\varphi = (\dot{m}_2 b_2 - \dot{m}_3 b_3)/6N - dA_w/d\varphi + dA_L/d\varphi + dA_f/d\varphi - dI/d\varphi. \tag{12}$$

The terms on the r.h.s. of Eq. (12) have the following meanings:

$$dA_w/d\varphi = (p - p_O)(dV/d\varphi) \tag{13}$$

is the work transfer, where $dV/d\varphi$ is the rate of change of cylinder volume with crank angle [2,5];

$$dA_L/d\varphi = (dQ_L/d\varphi)[1 - (T_0/T_g)] \tag{14}$$

is the heat transfer to the cylinder walls with $dQ_L/d\varphi$ given by the Annand correlation [Eq.(4)], and T_g the instantaneous cylinder gas temperature;

$$dA_f/d\varphi = (dm_{fb}/d\varphi)a_{fch}, \tag{15}$$

where a_{fch} is the availability associated with burning for liquid hydrocarbon fuels of the type C_mH_n and is given by [13]

$$a_{fch} = LHV[1.04224 + 0.011925(n/m) - 0.042/m]. \tag{16}$$

For the present analysis, $m = 12$, $n = 26$ and $a_{fch} = 1.064\,LHV$. The fuel burning rate $dm_{fb}/d\varphi$ is given by the Whitehouse–Way model [Eq. (2a) or (2b)]. The term on the l.h.s. of Eq. (12) is represented explicitly by

$$dA_{cyl}/d\varphi = dU/d\varphi + p_O(dV/d\varphi) - T_0(dS/d\varphi) - dG_0/d\varphi \tag{17}$$

and is the change in availability of the cylinder contents, with U denoting the internal energy (J), S the entropy (J/K), G the Gibbs free enthalpy (J), and V the instantaneous cylinder volume (m^3). Details concerning the derivation of the terms U, S and G_0 may be found in Refs. [5] and [16]. The terms $\dot{m}_2 b_2$ and $\dot{m}_3 b_3$ in Eq. (12) refer to the inflowing and outflowing exergy, respectively, where the flow availability is [13,29]

$$b = h - h_0 - T_0(s - s_0). \tag{18}$$

The term $dI/d\varphi$ in Eq.(12) is the rate of irreversibility production within the cylinder which consists mainly of the combustion term, while inlet-valve throttling and mixing of the incoming air with the cylinder residuals contribute a little [5,22].

For the inlet manifold, the exergy-balance equation is [5,22]

$$dA_{im}/d\varphi = (\dot{m}_1 b_1 - \dot{m}_2 b_2)/6N - dI_{im}/d\varphi, \tag{19}$$

where b_1 is the flow availability at the intake-manifold inlet evaluated at atmospheric conditions. The term for irrevesibilities $dI_{im}/d\varphi$ accounts for mixing of atmospheric air with the intake manifold contents.

For the exhaust manifold, the exergy-balance equation is [5,22]

$$dA_{em}/d\varphi = (\dot{m}_3 b_3 - \dot{m}_4 b_4)/6N - dI_{em}/d\varphi + dA_{L_{em}}/d\varphi, \tag{20}$$

where the index 3 denotes exit conditions from the engine cylinder and the index 4 identifies the exhaust manifold state. The term $dA_{L_{em}}/d\varphi = (dQ_{L_{em}}/d\varphi)[1 - (T_0/T_{em})]$ accounts for heat losses at the exhaust manifold, where T_{em} is the instantaneous temperature of the manifold contents. The term $dI_{em}/d\varphi$ is the irreversibility rate in the exhaust manifold, which arises from throttling across the exhaust valve, mixing of cylinder exhaust gases with manifold contents and friction along the manifold length. The terms $dA_{em}/d\varphi$ and $dA_{im}/d\varphi$ in Eqs. (20) and (19), respectively, are evaluated according to Eq. (17); for unsteady operations, they do not sum to zero (as they do for steady-state operation) at the end of a full cycle of the working medium. Their respective cumulative values $\int_0^{720} (dA/d\varphi)d\varphi$ are, however, small compared to the other availability terms, due to the natural aspiration operation of the engine.

RESULTS AND DISCUSSION

Equation (7) describes the energy balance at the crankshaft and Eqs. (12), (19) and (20) describe the exergy balances in the cylinder, inlet and exhaust manifolds, respectively. They have been applied for various schedules of speed and load changes and the results are given in Figs. 1–8. The engine under study is a naturally aspirated, indirect injection, Ricardo E-6 research diesel engine the technical characteristics of which are given in Table 1.

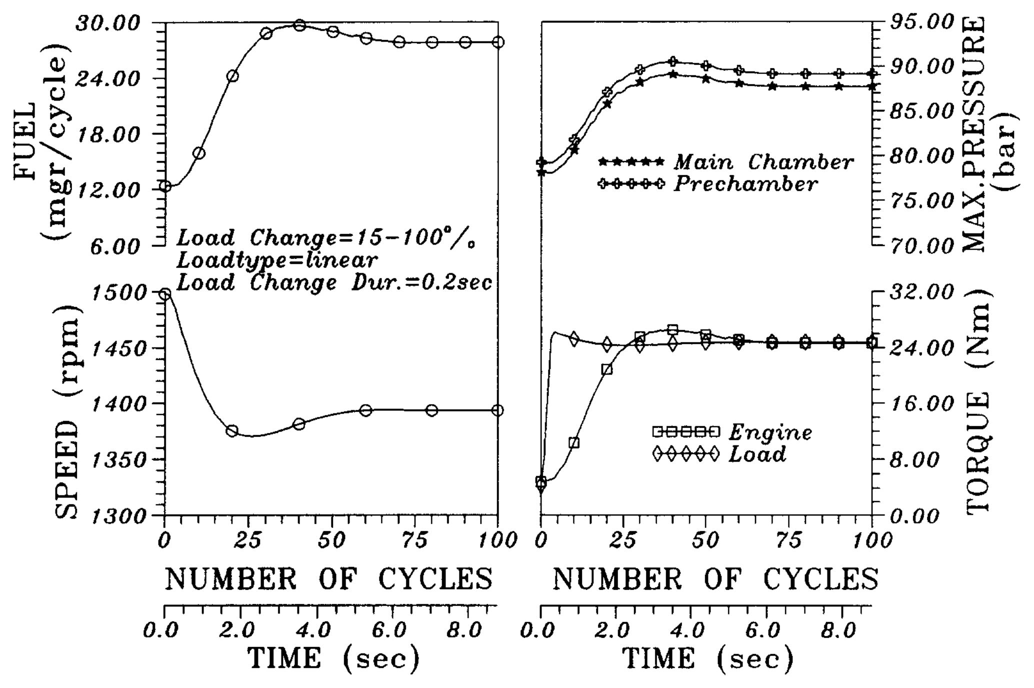

Fig. 1. Predicted engine energy response to an increase in load.

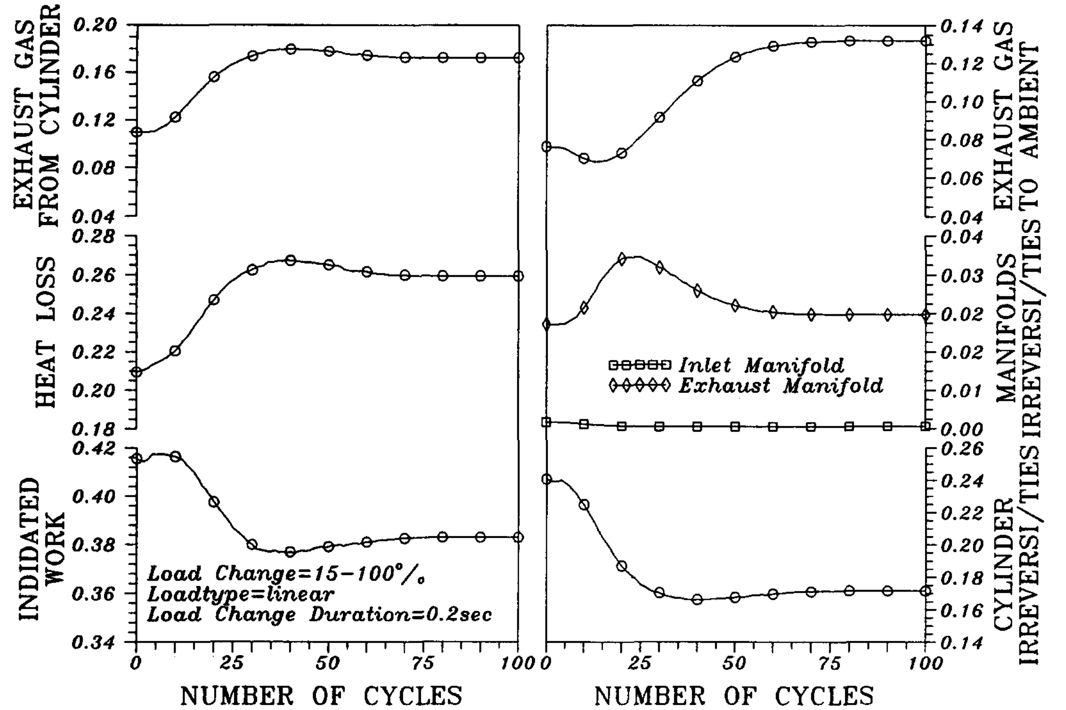

Fig. 2. Predicted engine exergy response to an increase in load.

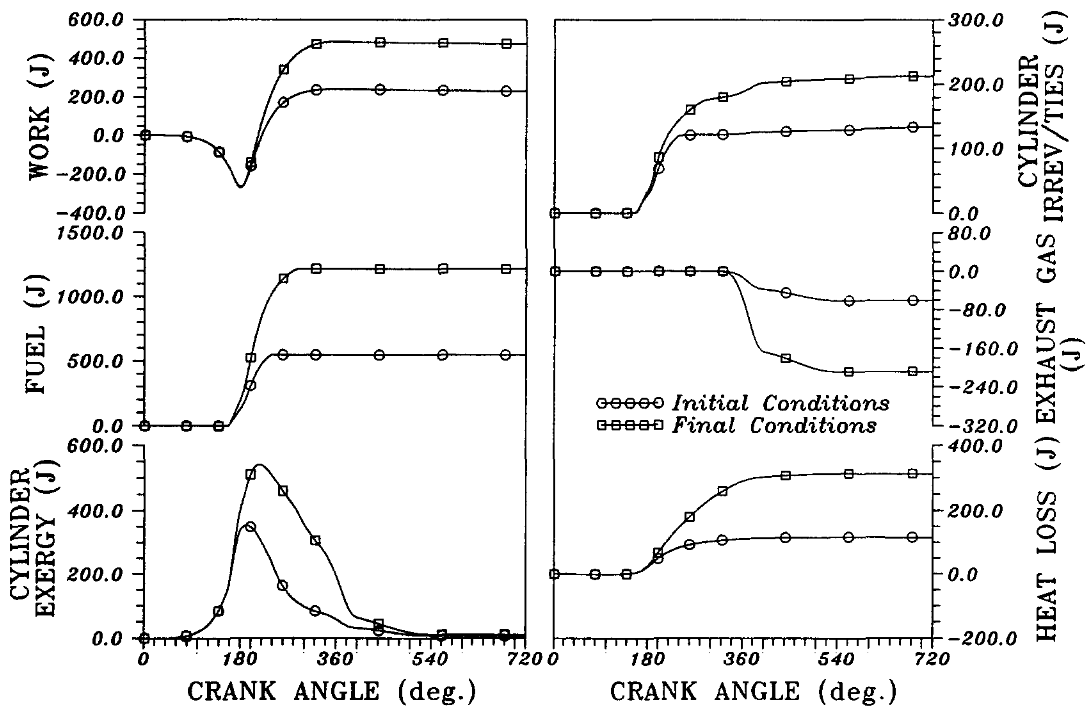

Fig. 3. Developments in the cumulative exergy terms of diesel engine at the initial and final steady-state conditions, after an increase in load.

Figures 1–5 refer to load changes which are characterized by the following data: (a) the initial load is 15% of the full engine load at the initial speed of 1500 rpm; (b) the full engine load (100%) at 1500 rpm is applied within 0.2 s; and (c) the load type is linear with a total moment of inertia G_{tot} = 1.5 kg-m^2.

Figure 1 is a presentation of predicted engine responses for speed, injected fuel, engine and load

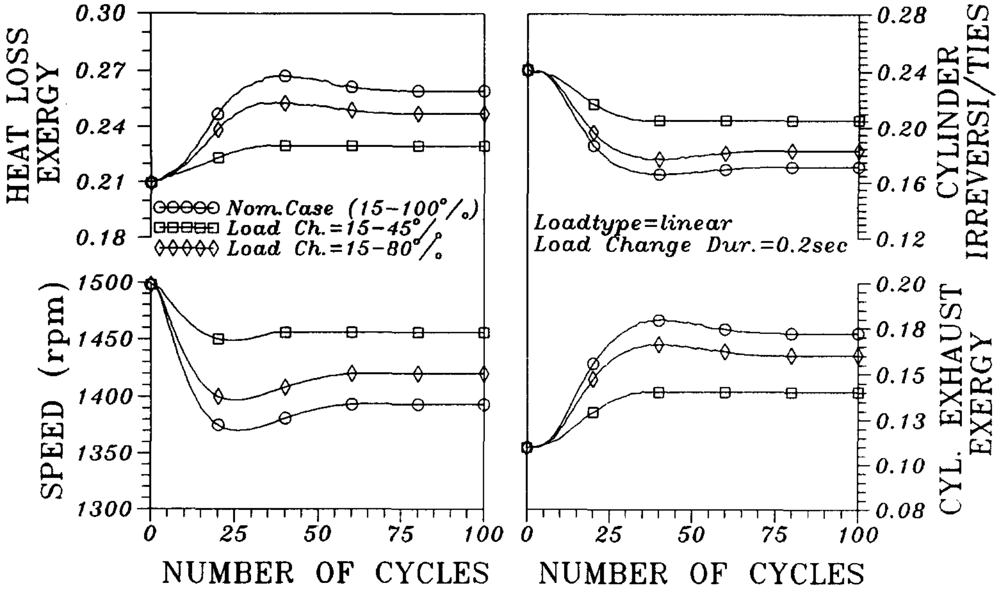

Fig. 4. Effect of the applied load-change intensity on engine speed and exergy-term responses as functions of the number of engine cycles.

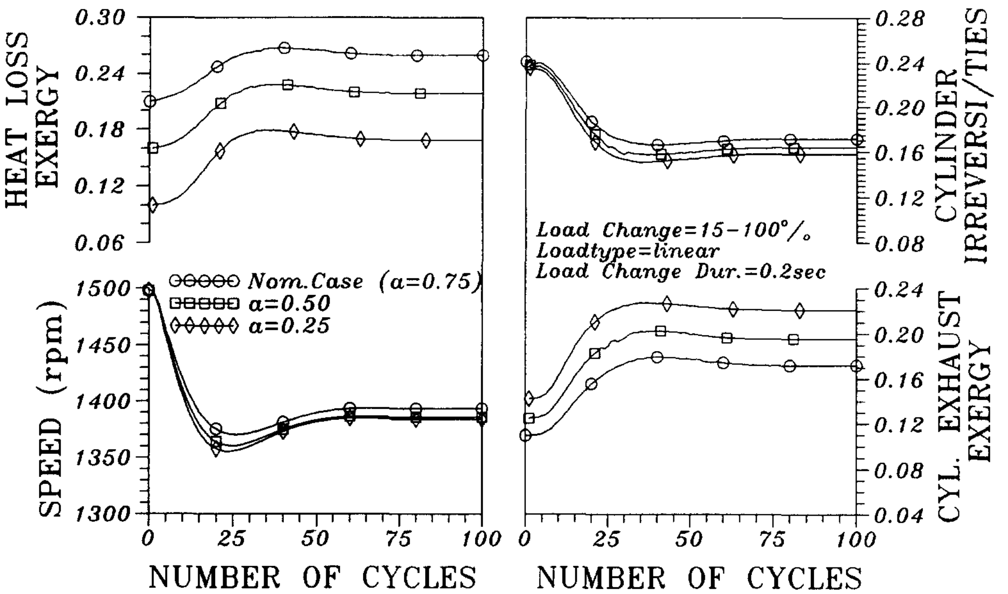

Fig. 5. Effect of the heat loss to the walls intensity on engine speed and exergy-term responses as functions of the number of engine cycles, after an increase in load.

torques, and maximum cylinder pressures (main chamber and prechamber) to nominal load changes. At the initial condition, the engine and load torques are equal. As soon as the new load is applied, the engine speed drops because the load torque becomes considerably greater than its engine counterpart. This imbalance leads to a movement of the governor towards a position of more fuelling. Because the load type is linearly related to speed, the load torque decreases with speed, resulting in a rapid counter-balance between engine and load.

Figure 2 shows the responses of the exergy terms, viz., indicated work, heat loss to the walls, exhaust gas from the cylinder, exhaust-manifold gas to the ambient, cylinder irreversibilities, and inlet- and exhaust-manifold irreversibilities as functions of the cycles. All of these terms are cumulative values over each cycle, divided by the chemical availability of the current cycle fuel. The exergy terms for heat losses to the walls increase as functions of the number of engine cycles because of increases in the charge temperatures resulting from increases of the injected fuel quantities and accompanying fuel–

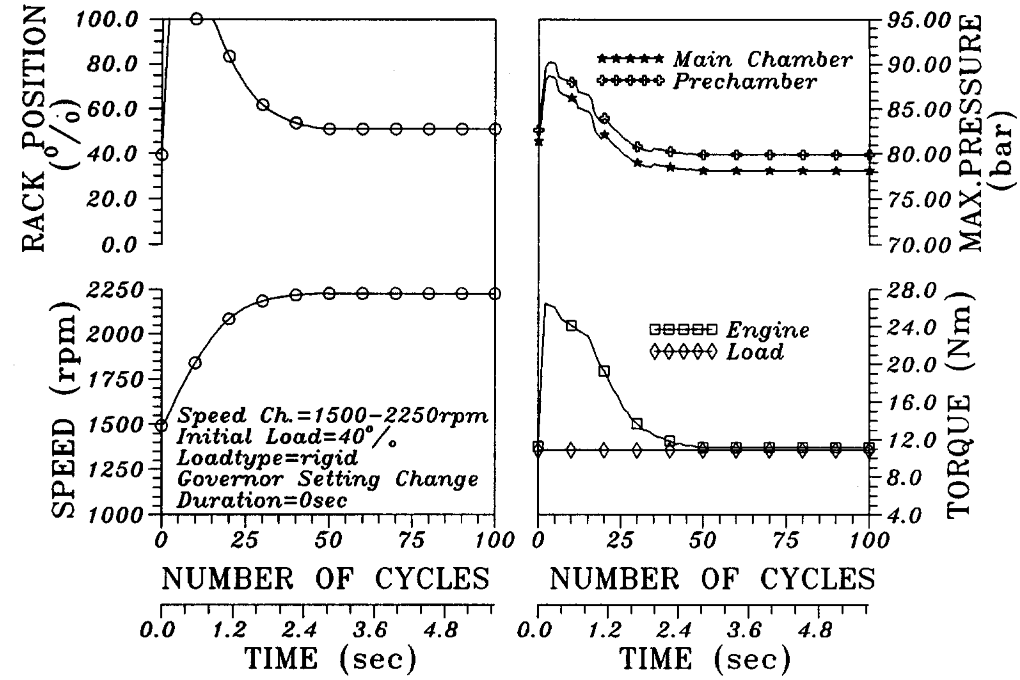

Fig. 6. Predicted engine energy response to a ramp increase in governor setting.

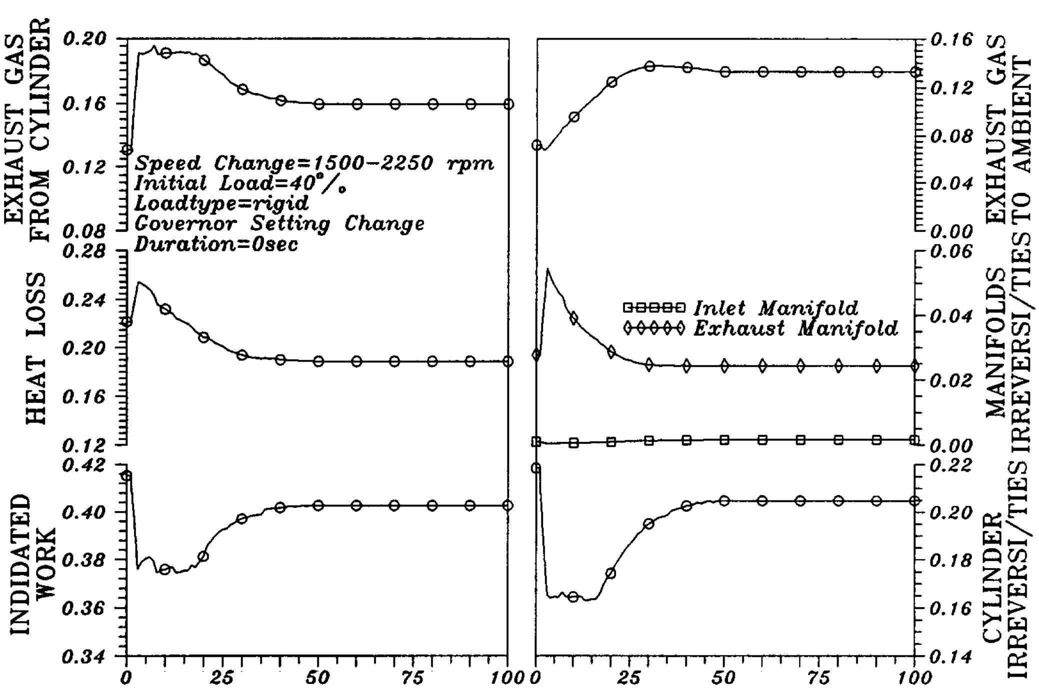

Fig. 7. Predicted engine exergy response to a ramp increase in governor setting.

air equivalence ratios f; similar results hold for the two exhaust-gas terms. All of the specified properties have profiles similar to the fuel term in Fig. 1.

Cylinder (combustion) irreversibilities decrease as the transient events proceed due to the fact that combustion irreversibilities fall with increasing loads. Greater loads result in less degradation of fuel chemical availability when transferred to the exhaust gases and also less mixing of exhaust gases with the air. The inlet-manifold irreversibilities constitute a very small percentage of the fuel chemical avail-

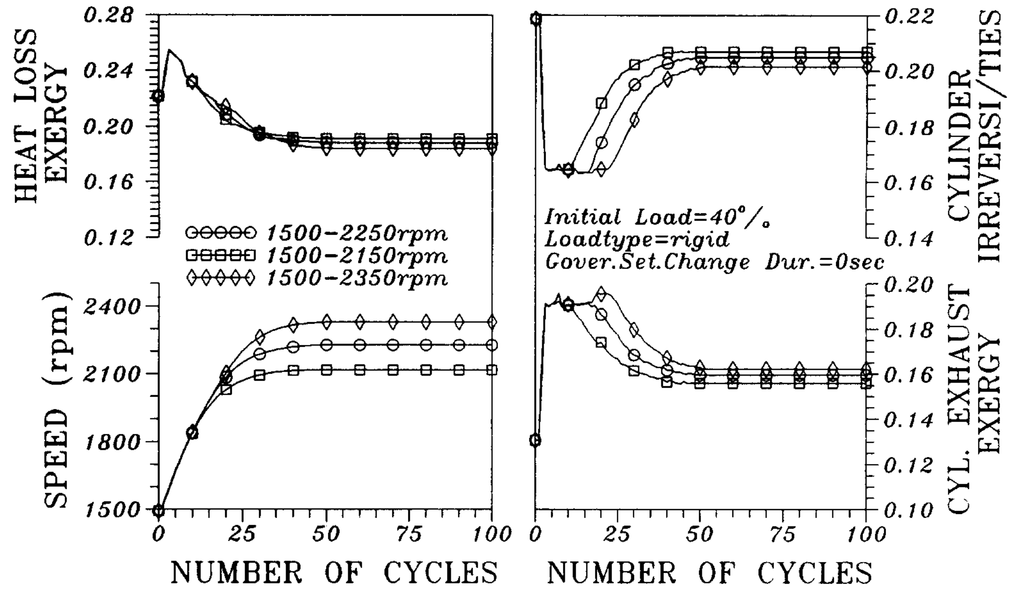

Fig. 8. Effect of the speed-changes intensity on exergy-term developments as functions of the number of engine cycles, after a ramp increase in governor setting.

Table 1. Basic design data for a Ricardo E-6 research diesel engine.

Type	Single-cylinder, four-stroke, IDI
Bore	76.2 mm
Stroke	111.2 mm
Connecting rod length	240.5 mm
Compression ratio	21.29
Prechamber volume	11.5 cm^3
Main chamber dead volume	13.5 cm^3
Inlet valve opening	8°CA before top dead center
Inlet valve closure	36°CA after bottom dead center
Exhaust valve opening	43°CA before bottom dead center
Exhaust valve closure	7°CA after top dead center
Static injection timing	38°CA before top dead center

ability, whereas those for the exhaust manifold increase substantially between cycles 10 and 30 for which the main increase in injected fuel quantity occurs.

Figure 3 is focused on the first and last cycles of the particular transient operation and shows the differentiation in the development of the various cumulative exergy terms.

Figure 4 indicates the effect of the intensity of applied-load changes on speed and cylinder exergy-term responses. The load changes affect the speed responses strongly and consequently also the fuel responses (not shown in Fig. 4), which in turn affect all of the second-law terms considerably. The reduced combustion irreversibilities decrease with increases in the injected fuel quantity, whereas the heat losses to the walls and the exhaust-gas terms increase as a percentage of the fuel chemical availability.

Figure 5 shows the effect of the intensity of heat losses to the walls, described through the coefficient a of the Annand relation [Eq.(4)], on the speed and cylinder exergy-term responses of the engine. Greater values of the coefficient a result in an increase in the heat losses to the walls and in lower charge temperatures. As far as the engine-speed responses are concerned, no particular difference is observed between the three examined a values. The exergy terms for heat losses to the walls decrease substantially with decreasing a, the exergy term for the exhaust gases increases with decreasing a due to subsequent increases in the charge temperatures, while the combustion irreversibilities remain essentially unaltered and confirm remarks made in Ref. [19].

Figures 6–8 show the responses of the first- and second-law terms after a ramp increase in governor setting during an acceleration event and for a constant engine load equal to 40%, while the total moment of inertia G_{tot} = 0.30 kg-m^2 is typical for an automotive application with intermediate gear. The fuel-pump rack position reaches its maximum value instantly with a change in the governor setting, which results in an almost linear increase in speed. The speed is then maintained until a final value of 2250 rpm is reached before it drops so that dynamic equilibrium may also achieved.

Figure 7 shows the responses of the reduced exergy terms as functions of the number of engine cycles which, with the exception of the responses of the exhaust-manifold gases to the ambient term, show similar temporal changes with fuel-pump rack position or fuel (cf. Fig. 6). It is interesting to note that the indicated work, heat loss to the walls and combustion-irreversibility terms equilibrate at lower final values, whereas each of the two exhaust-gas terms equilibrates at a final value higher than the initial value.

Figure 8 shows three different accelerating events, all commencing from 1500 rpm. The increases in final speed decrease the reduced amount of heat lost to the walls (due to the relatively short time available for heat exchange) and the combustion-irreversibility terms, while the exhaust-gas terms increase mainly because of slightly greater amounts of injected fuel during transient events.

CONCLUSIONS

A detailed first- and second-law analysis has been performed on a single-cylinder, naturally-aspirated, indirect-injection diesel engine to study the energy and exergy performance of engine subsystems during various transient operating schedules comprising changes in speed and load. We conclude that combustion irreversibilities decrease after a ramp increase in load, whereas the intensity of the heat lost to the walls has a minimal effect on the combustion irreversibilities. The indicated work decreases after both speed or load increases. Furthermore, the exergy terms for the heat losses to the walls increase after an increase in load, which becomes especially clear the greater the heat loss to the walls becomes. However, an increase in speed under a constant load reduces the relative value of the exergy terms for heat losses. The exergy terms for the exhaust gases from the cylinder and for the exhaust-manifold gas to the ambient increase with increasing load or speed and also with decreasing heat loss to the walls. The exhaust-manifold irreversibilities vary strongly during a load or speed change, while the inlet-manifold irreversibilities are insignificant.

NOMENCLATURE

A = Availability or exergy (J)
a = Specific availability or specific exergy (J/kg)
b = Flow availability (J/kg)
f = Fuel–air equivalence ratio
h = Specific enthalpy (J/kg)
I = Irreversibility (J)
M,m = Mass (kg)
N = Engine speed (rpm) or force (N)
p = Pressure (Pa)
Q = Heat (J)
s = Specific entropy (J/kg K)
T = Absolute temperature (K), or torque = (Nm)
t = Time (s)

Greek symbols

φ = Crank angle (deg or rad)
ω = Angular velocity (s^{-1})

Subscripts

0,1 = Atmosphere or initial conditions
2 = Inlet manifold
3 = Cylinder
4 = Exhaust manifold
b = Burned
ch = Chemical
f = Fuel
i = Injected
g = Gas
L = Load or loss
w = Wall or work

Abbreviations

CA = Crank angle (degrees)
rpm = Revolutions per minute

REFERENCES

1. Ferguson, C. R., *Internal Combustion Engines*. Wiley, New York, 1986.
2. Heywood, J. B., *Internal Combustion Engine Fundamentals*. McGraw-Hill, New York, 1988.
3. Benson, R. S. and Whitehouse, N. D., *Internal Combustion Engines*. Pergamon Press, Oxford, 1979.

4. Kouremenos, D. A., Rakopoulos, C. D. and Hountalas, D. T., *Trans. ASME, J. Engng Gas Turbines Power*, 1990, **112**, 138.
5. Rakopoulos, C. D. and Giakoumis, E. G., *Energy Convers. Mgmt*, 1997, **38**, 347.
6. Watson, N. and Marzouk, M., A non-linear digital simulation of turbocharged diesel engines under transient conditions. SAE Paper No. 770123, Society of Automotive Engineers, Inc., Warrendale, PA, 1977.
7. Watson, N., Transient performance simulation and analysis of turbocharged diesel engines. SAE paper No. 810338, Society of Automotive Engineers, Inc., Warrendale, PA, 1981.
8. Horlock, J. H. and Winterbone, D. E., *The Thermodynamics and Gas Dynamics of Internal Combustion Engines*, Vol. II. Clarendon Press, Oxford, 1986.
9. Gardner, T. P. and Henein, N. A., Diesel starting: a mathematical model. SAE Paper No. 880426, Society of Automotive Engineers, Inc., Warrendale, PA, 1988.
10. Bazari, Z., Diesel exhaust emissions prediction under transient operating conditions. SAE paper No. 940666, Society of Automotive Engineers, Inc., Warrendale, PA, 1994.
11. Rakopoulos, C. D., Giakoumis, E. G. and Hountalas, D. T., A simulation analysis of the effect of governor technical characteristics and type on the transient performance of a naturally aspirated IDI diesel engine. SAE paper No. 970633, Society of Automotive Engineers, Inc., Warrendale, PA, 1997.
12. Rakopoulos, C. D., Hountalas, D. T., Mavropoulos, G. C. and Giakoumis, E. G., An integrated transient analysis simulation model applied in thermal loading calculations of an air-cooled diesel engine. SAE paper No. 970634, Society of Automotive Engineers, Inc., Warrendale, PA, 1997.
13. Moran, M. J. and Shapiro, H. N., *Fundamentals of Engineering Thermodynamics*. Wiley, New York, 1992.
14. Flynn, P. F., Hoag, K. L., Kamel, M. M. and Primus, R. J., A new perspective on diesel engine evaluation based on second law analysis. SAE Paper No. 840032, Society of Automotive Engineers, Inc., Warrendale, PA, 1984.
15. Primus, R. J., Hoag, K. L., Flynn, P. F. and Brandts, M. C., An appraisal of advanced engine concepts using second law analysis techniques. SAE Paper No. 841287, Society of Automotive Engineers, Inc., Warrendale, PA, 1984.
16. Van Gerpen, J. H. and Shapiro, H. N., *Trans. ASME, J. Engng Gas Turbines Power*, 1990, **112**, 129.
17. Dunbar, W. R. and Lior, N., Teaching power cycles by both first-and-second law analysis of their evolution. *Proc. ASME-WAM*, AES Vol. 27, Anaheim, CA, November, 1992.
18. Bozza, F., Nocera, R., Senatore, A. and Tuccilo, R., Second law analysis of turbocharged engine operation. SAE Paper No. 910418, Society of Automotive Engineers, Inc., Warrendale, PA, 1991.
19. Rakopoulos, C. D. and Andritsakis, E. C., DI and IDI combustion irreversibility analysis. *Proc. ASME-WAM*, AES Vol. 30/HTD Vol. 266, New Orleans, LA, 1993.
20. Rakopoulos, C. D., Andritsakis, E. C. and Kyritsis, D. K., *Heat Recov. Syst. CHP*, 1993, **13**, 261.
21. Rakopoulos, C. D., *Energy Convers. Mgmt*, 1993, **33**, 1299.
22. Rakopoulos, C. D. and Giakoumis, E. G., *Applied Thermal Engng*, 1997, **17**, 299.
23. Obert, E. F. and Gaggioli, R. A., *Thermodynamics*. McGraw-Hill, New York, 1963.
24. Krieger, R. B. and Borman, G. L., The computation of apparent heat release for internal combustion engines. ASME Paper No. 66 WA/DGP-4, 1966.
25. Millington, B. W. and Hartles, E. R., Frictional losses in diesel engines. SAE Paper No. 680590, Society of Automotive Engineers, Inc., Warrendale, PA, 1968.
26. Taylor, C. F., *The Internal Combustion Engine in Theory and Practice*, Vol. 2. MIT Press, Cambridge, MA, 1985.
27. Krutov, V. I., *Automatic Control of Internal Combustion Engines*. MIR Publishers, Moscow, 1987.
28. Welbourne, D. B., Roberts, D. K. and Fuller, R. A., *Proc. Inst. Mech. Engrs.*, 1959, **173**, 575.
29. Bejan, A., *Advanced Engineering Thermodynamics*. Wiley, New York, 1988.
30. Bejan, A., Tsatsaronis, G. and Moran, M., *Thermal Design and Optimization*. Wiley, New York, 1996.
31. Boehm, R. F., *Design Analysis of Thermal Systems*. Wiley, New York, 1987.
32. Gyftopoulos, E. P. and Beretta, G. P., *Thermodynamics: Fundamentals and Applications*. Macmillan, New York, 1991.